Higgs Physics at the LHC and Beyond: Connecting Colliders and the Early Universe

DeCAF Seminar, U. Autónoma de Madrid

April 15 2026

Thomas Biekötter

thomasbiekoetter thomas.biekoetter

The Higgs boson in the SM

The SM Higgs sector is a **minimal parametrisation** of EW symmetry breaking

$\to$ **one fundamental scalar particle** with well defined properties (once its mass is known)

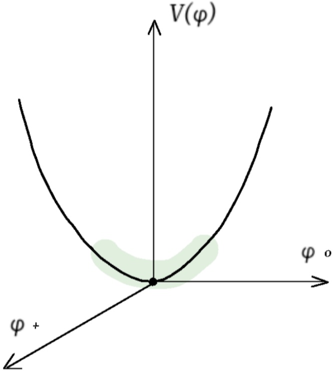

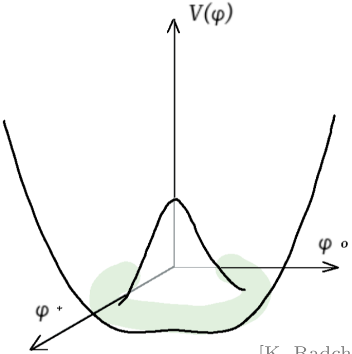

[K. Radchenko, PhD thesis]

$$\mathcal{L}_\Phi = (D_\mu \Phi)^\dagger (D^\mu \Phi) + V(\Phi) + \mathcal{L}_{\text{Yukawa}} \qquad V(\Phi) = -\mu^2 \, \Phi^\dagger \Phi + \lambda (\Phi^\dagger \Phi)^2$$

The Higgs boson in the SM

The SM Higgs sector is a **minimal parametrisation** of EW symmetry breaking

→ **one fundamental scalar particle** with well defined properties (once its mass is known)

Striking predictions:

1. Couplings scale with particle mass (squared)

$$Y_{ij}\bar{\psi}^i_L H \psi^j_R \quad \to \quad M^{\psi}_{ij} \sim v Y_{ij}$$

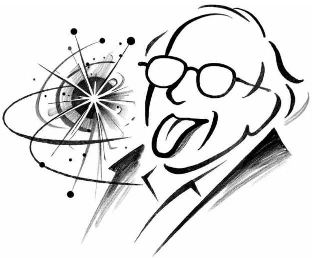

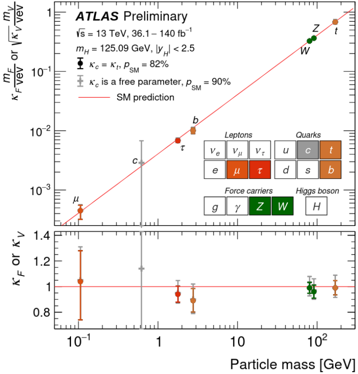

[ATLAS-CONF-2025-006]

The Higgs boson in the SM

The SM Higgs sector is a **minimal parametrisation** of EW symmetry breaking

$\rightarrow$ **one fundamental scalar particle** with well defined properties (once its mass is known)

Striking predictions:

1. Couplings scale with particle mass (squared)

2. No (tree-level) flavour changing couplings

$$Y_{ij}\bar{\psi}_L^i H \psi_R^j \quad \rightarrow \quad M_{ij}^{\psi} \sim v Y_{ij}$$

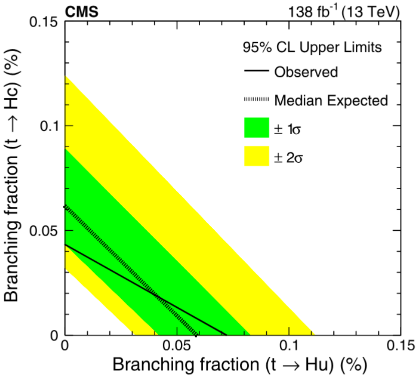

[CMS, 2407.15172]

The Higgs boson in the SM

The SM Higgs sector is a **minimal parametrisation** of EW symmetry breaking

$\rightarrow$ **one fundamental scalar particle** with well defined properties (once its mass is known)

Striking predictions:

1. Couplings scale with particle mass (squared)

2. No (tree-level) flavour changing couplings

3. Custodial symmetry implies

$$\rho = \frac{M_W^2}{M_Z^2 \cos^2\theta_W} = 1 \text{ at tree level}$$

$$\rho^{\text{exp}} \approx 1.00031 \pm 0.00019$$

[PDG (2024)]

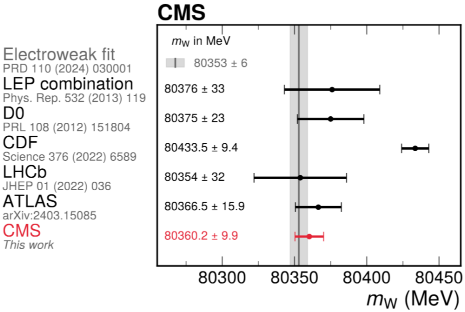

[CMS, 2412.13872]

The Higgs boson in the SM

The SM Higgs sector is a **minimal parametrisation** of EW symmetry breaking

→ **one fundamental scalar particle** with well defined properties (once its mass is known)

Striking predictions:

1. Couplings scale with particle mass (squared)
2. No (tree-level) flavour changing couplings
3. Custodial symmetry implies
   $\rho = \frac{M_W^2}{M_Z^2 \cos^2\theta_W} = 1$ at tree level
4. Absence of CP violation in the Higgs potential

$$\left[\Phi^\dagger\Phi + \text{h.c.}\right]^\dagger = \Phi^\dagger\Phi + \text{h.c.}$$

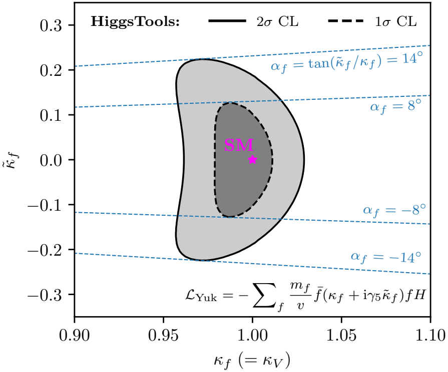

The Higgs boson in the SM

The SM Higgs sector is a **minimal parametrisation** of EW symmetry breaking

$\rightarrow$ **one fundamental scalar particle** with well defined properties (once its mass is known)

Striking predictions:

1. Couplings scale with particle mass (squared)
2. No (tree-level) flavour changing couplings
3. Custodial symmetry implies
   $\rho = \frac{M_W^2}{M_Z^2 \cos^2 \theta_W} = 1$ at tree level
4. Absence of CP violation in the Higgs potential
5. There was no electroweak phase transition in the early universe

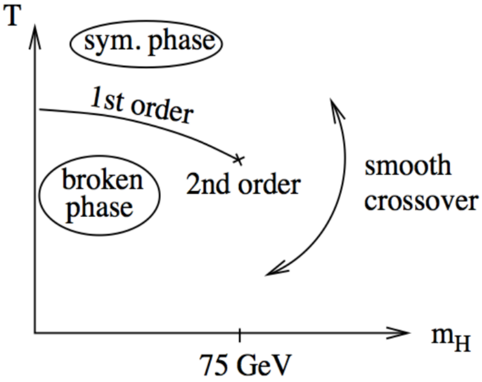

[Rummukainen et al, hep-lat/9805013]

The Higgs boson as a portal to new phenomena

"It is precisely the simple hypotheses that one must be most wary of, because they are the ones most likely to go unnoticed."

— ***Henri Poincaré***

"C'est même des hypothèses simples qu'il faut le plus se défier, parce que ce sont celles qui ont le plus de chances de passer inaperçues."

There are many motivations for **non-minimal/extended Higgs sector**:

- Matter-antimatter asymmetry of the universe → **EW baryogenesis**
- Dark matter → Higgs-portal dark matter
- Flavour problem and the hierarchy of fermion masses
- Neutrino masses
- ...

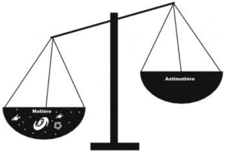

[Credits: GANIL]

With additional scalars, many appealing SM features are **no longer automatic**

→ **The Higgs sector is an ideal testbed for physics beyond the SM**

125 GeV Higgs boson: The stress test

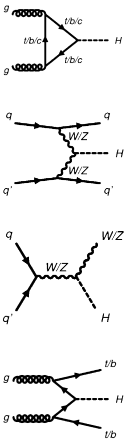

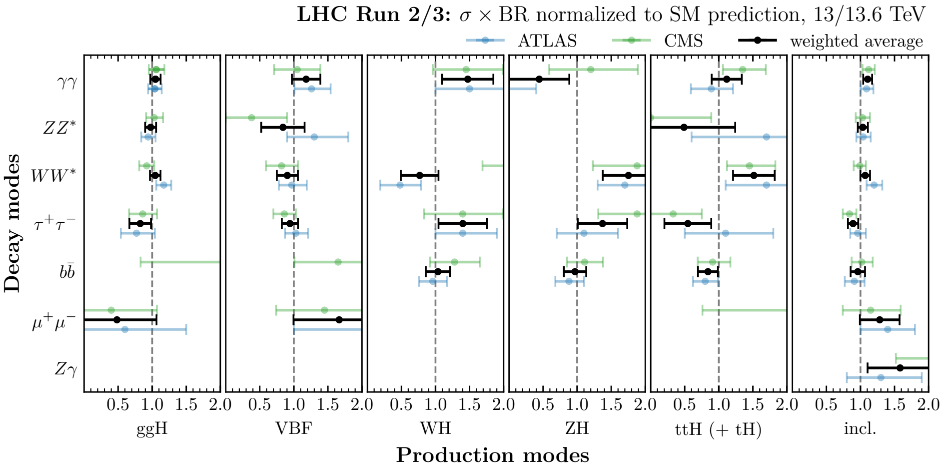

Data: [CMS-PAS-HIG-21-018] [ATLAS-CONF-2025-006] [CMS, 2509.22535] [ATLAS, 2207.00092] [ATLAS and CMS, 2309.03501]

125 GeV Higgs boson: The stress test

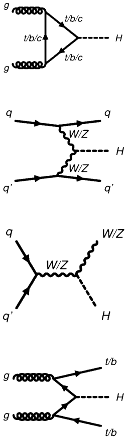

LHC Run 2/3: $\sigma \times \mathrm{BR}$ normalized to SM prediction, 13/13.6 TeV

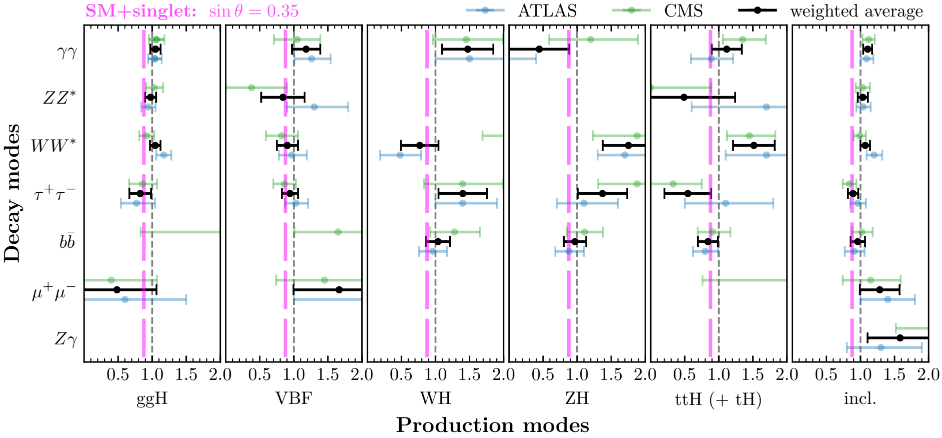

Data: [CMS-PAS-HIG-21-018] [ATLAS-CONF-2025-006] [CMS, 2509.22535] [ATLAS, 2207.00092] [ATLAS and CMS, 2309.03501]

125 GeV Higgs boson: The stress test

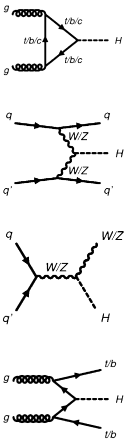

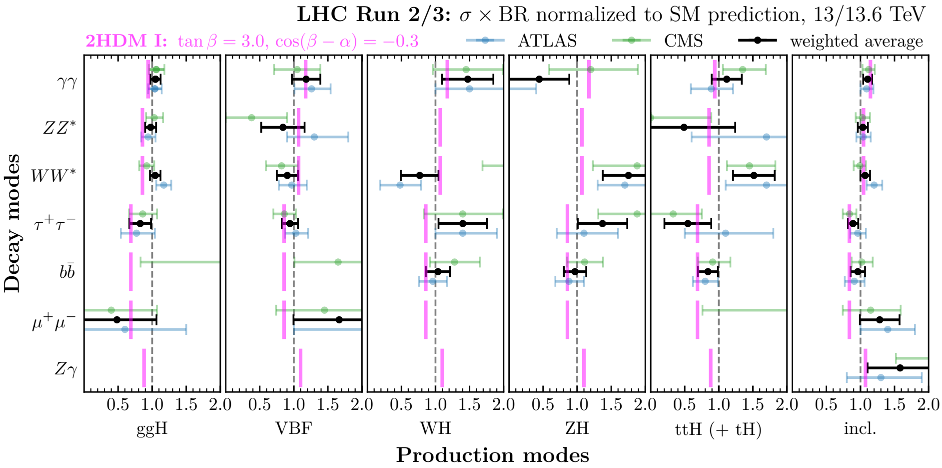

Data: [CMS-PAS-HIG-21-018] [ATLAS-CONF-2025-006] [CMS, 2509.22535] [ATLAS, 2207.00092] [ATLAS and CMS, 2309.03501]

Baryon asymmetry of the universe (BAU)

Baryon-to-photon ratio:

[van de Vis, de Vries, Postma, 2508.09989]

$$Y_b = \frac{1}{7.04} \frac{n_b - \bar{n}_b}{n_\gamma} = \begin{cases} (8.2 - 9.4) \cdot 10^{-11} \text{ from BBN} \\ (8.65 \pm 0.09) \cdot 10^{-11} \text{ from CMB (Planck)} \end{cases}$$

Power spectrum of the CMB

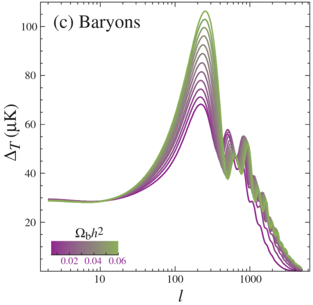

[Wayne Hu et al, astro-ph/0110414]

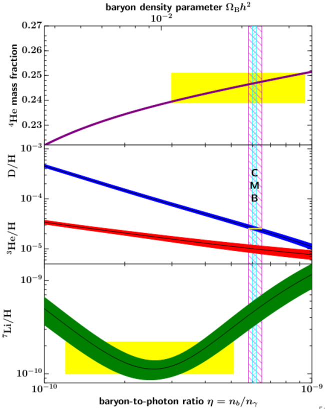

[PDG (2022)]

* Also no observations pointing to confined pockets of antimatter in the universe, e.g. radiation from anti-stars or anti-galaxies.

The 3 Sakharov conditions

1. Baryon number violation

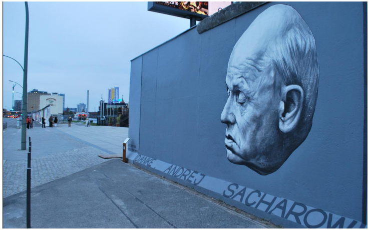

2. C and CP violation

3. Out of equilibrium

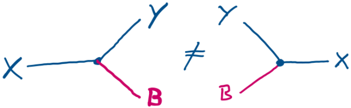

The 3 Sakharov conditions in the SM

1. Baryon number violation ✓

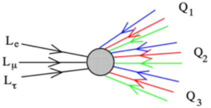

Sphaleron process, active at $T \gtrsim v$

[Klinkhammer et al. (1984), Kuzmin et al. (1985)]

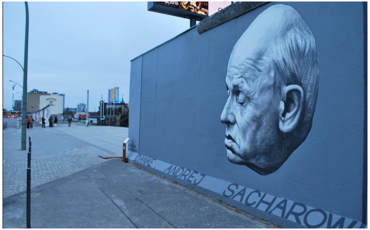

2. C and CP violation (✗)

CP violation from CKM:

$$\Rightarrow \eta \sim 10^{-20}$$

(assuming strong EWPT)

[Gavela et al, hep-ph/9312215]

3. Out of equilibrium ✗

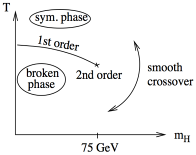

"...there is no EWPT in the SM."

[Rummukainen et al, hep-lat/9805013]

Strong 1st-order EW phase transition

Out-of-equilibrium dynamics in the early universe → **3. Sakharov condition ✓**

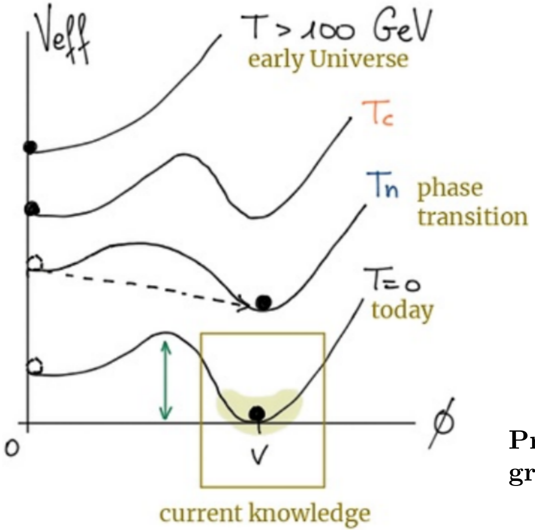

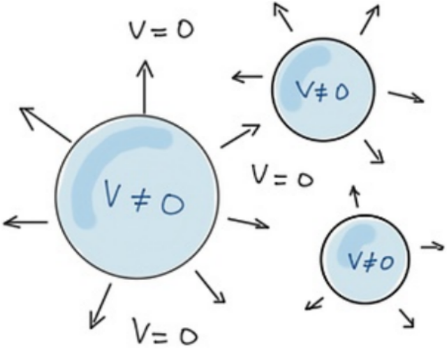

[Drawings by Kateryna Radchenko]

Primordial remnant: stochastic gravitational wave (GW) background

EWPT in perturbation theory

Loose categorization of different ways to realize an EWPT:

SM with $m_h \lesssim 60$ GeV

SMEFT with $C_H/\Lambda^2 \lesssim -2$

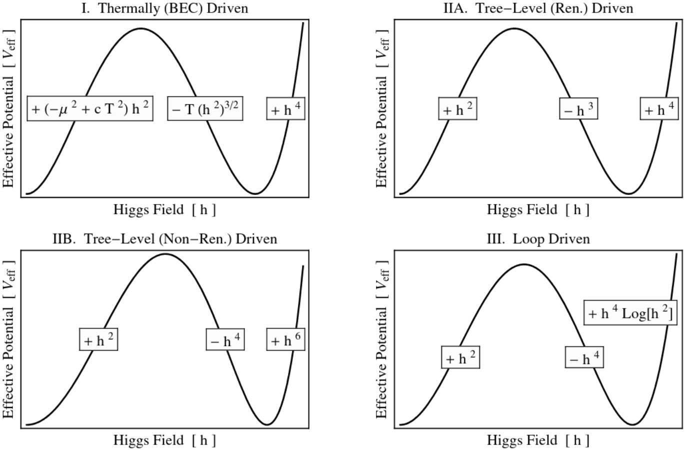

SM + singlet

2HDM

[Chung et al, hep-ph/1209.1819]

Electroweak baryogenesis

A mechanism to **dynamically generate the baryon asymmetry of the universe (BAU)**

[Dimopoulos, Susskind (1978)], [Kuzmin, Rubakov, Shaposhnikov (1985)]

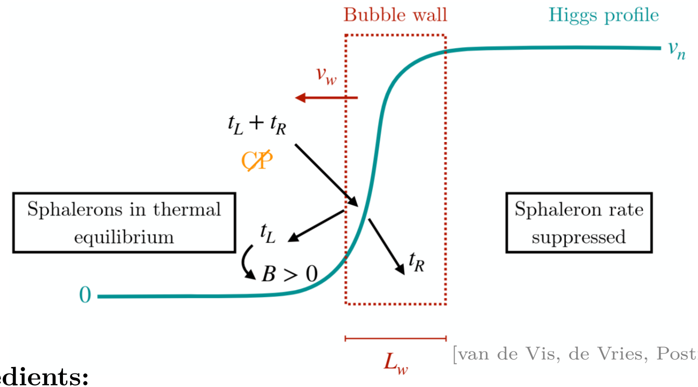

[van de Vis, de Vries, Postma, 2508.09989]

Required BSM ingredients:

1. Strong 1st-order EWPT with $v/T \gtrsim 1$
2. New sources of CP violation

New physics at the EW scale → EW baryogenesis is a collider target

Electroweak baryogenesis

A mechanism to **dynamically generate the baryon asymmetry of the universe (BAU)**

[Dimopoulos, Susskind (1978)], [Kuzmin, Rubakov, Shaposhnikov (1985)]

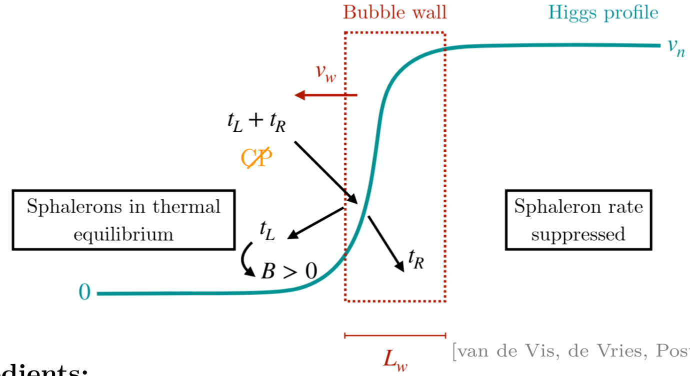

[van de Vis, de Vries, Postma, 2508.09989]

Required BSM ingredients:

1. Strong 1st-order EWPT with $v/T \gtrsim 1$
2. New sources of CP violation

New physics at the EW scale → EW baryogenesis is a collider target

Space-based GW astronomy

GW peak frequency: $f_{\text{peak}} \sim 1.6 \cdot 10^{-3}\ \text{Hz} \left(\frac{\beta/H}{100}\right) \left(\frac{T}{100\ \text{GeV}}\right) \left(\frac{g_*}{100}\right)^{1/6} \Rightarrow$ EWPT: $f_{\text{peak}} \sim 1$ mHz

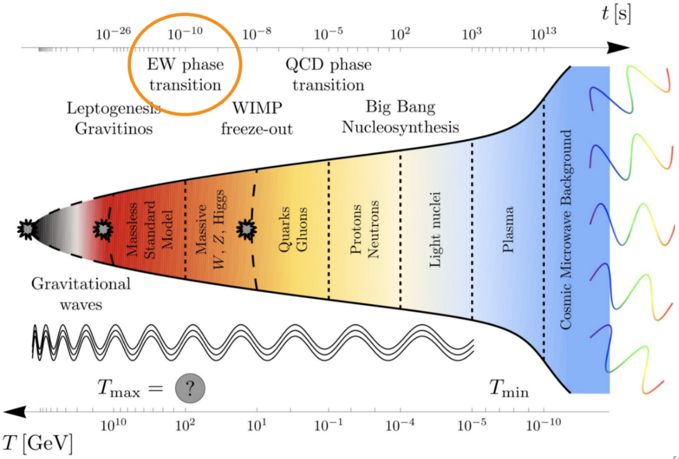

[K. Schmitz, 1307.3887]

Space-based GW astronomy

LISA will open a completely **new window into the early universe** at times before BBN

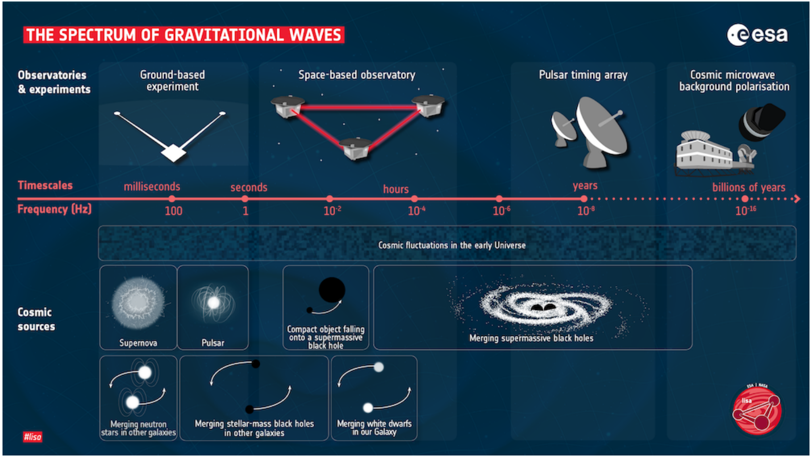

[ESA, Standard Licence]

Electron electric dipole moment (EDM)

It is shown that if Higgs-boson exchange mediates *CP* violation a significant electric dipole moment for the electron can result. Analogous effects can contribute to the neutron's electric dipole moment at a level competitive with Weinberg's three-gluon operator.

[Barr, Zee, PRL 65, 2920 (1990)]

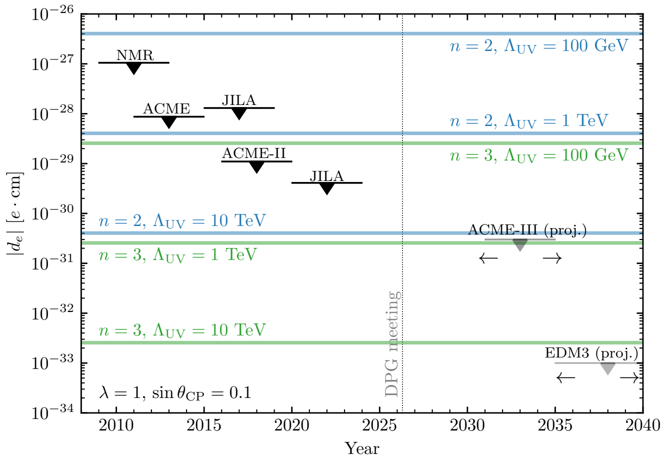

"Barr-Zee diagrams":

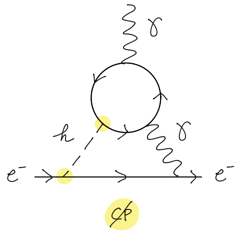

Estimate from dim. analysis:

$$\frac{|d_e|}{e} \sim \left(\frac{\lambda^2}{16\pi^2}\right)^n \frac{m_e}{\Lambda_{\text{UV}}} \sin\theta_{\text{CP}}$$

SM: $|d_e| \sim 10^{-35} e \cdot \text{cm}$

An EWPT in the 2HDM

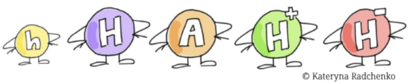

The 2HDM predicts two neutral BSM Higgs bosons H and A and a pair of charged Higgs bosons $H^\pm$
$\to$ **non-decoupling effects from mass splittings** between H and A $\to$ **strongest EWPT**

$$V_{\text{tree}}(\Phi_1,\Phi_2) = m_{11}^2\,\Phi_1^\dagger\Phi_1 + m_{22}^2\,\Phi_2^\dagger\Phi_2 - \left(m_{12}^2\Phi_1^\dagger\Phi_2 + \text{h.c.}\right) + \frac{1}{2}\lambda_1(\Phi_1^\dagger\Phi_1)^2 + \frac{1}{2}\lambda_2(\Phi_2^\dagger\Phi_2)^2$$
$$+\,\lambda_3(\Phi_1^\dagger\Phi_1)(\Phi_2^\dagger\Phi_2) + \lambda_4(\Phi_1^\dagger\Phi_2)(\Phi_2^\dagger\Phi_1) + \frac{1}{2}\left(\lambda_5(\Phi_1^\dagger\Phi_2)^2 + \text{h.c.}\right)$$

CP: $t_\beta = \dfrac{v_2}{v_1},\ M = \dfrac{m_{12}^2}{s_\beta c_\beta},\ v^2 = v_1^2 + v_2^2 = 246^2\ \text{GeV}^2,\ c_{\beta-\alpha},\ m_h,\ m_H,\ m_A,\ m_{H^\pm}$

Alignment limit: $c_{\beta-\alpha} = 0\ (m_h = 125\ \text{GeV})$

CPV: $t_\beta,\ M,\ v,\ \alpha_1,\ \alpha_3,\ m_{h_1},\ m_{h_2},\ m_{h_3},\ m_{H^\pm}$ (α_2 not a free parameter)

Alignment limit: $s_{\beta-\alpha_1} = 0\ (m_{h_1} = 125\ \text{GeV})$

CP violation: $\alpha_3 \neq 0, \pm\dfrac{\pi}{2}$

Details in [TB, Olea-Romacho, 2505.09670]

An EWPT in the 2HDM

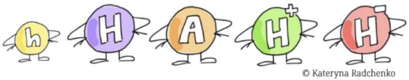

The 2HDM predicts two neutral BSM Higgs bosons H and A and a pair of charged Higgs bosons $H^{\pm}$
$\rightarrow$ **non-decoupling effects from mass splittings** between H and A $\rightarrow$ **strongest EWPT**

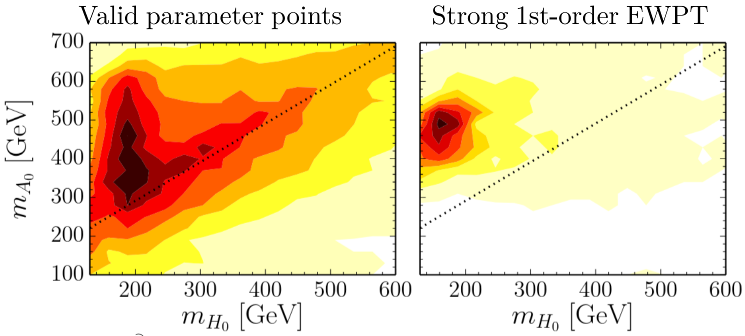

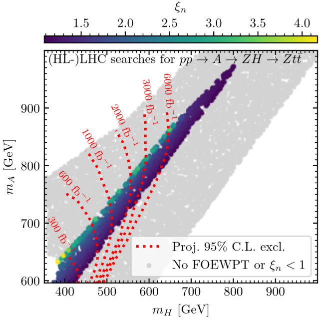

$m_H > 2 m_t$

[Dorsch, Huber, Mimasu, No, 1405.5537]

[TB, Heinemeyer, No, Olea-Romacho, Weiglein, 2208.14466]

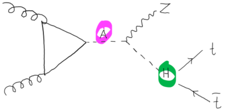

Multi-Higgs signatures become 'smoking-gun' signatures at the LHC
Increasing importance of **multi-top final states** after LHC Run 2

An EWPT in the 2HDM

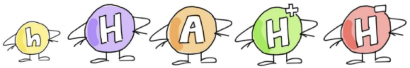

© Kateryna Radchenko

The 2HDM predicts two neutral BSM Higgs bosons H and A and a pair of charged Higgs bosons $H^{\pm}$
$\rightarrow$ **non-decoupling effects from mass splittings** between H and A $\rightarrow$ **strongest EWPT**

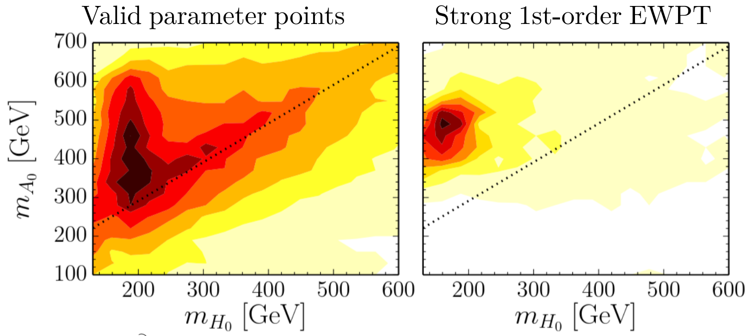

[Dorsch, Huber, Mimasu, No, 1405.5537]

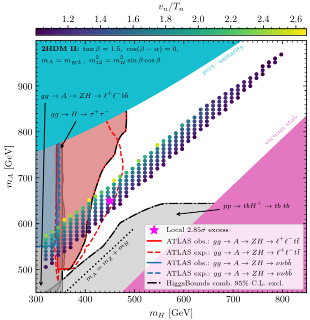

[TB, Heinemeyer, No, Olea-Romacho, Radchenko, Weiglein, 2309.17431]

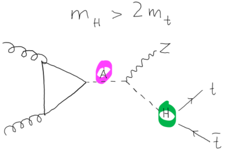

Multi-Higgs signatures become ‘smoking-gun’ signatures at the LHC

Increasing importance of **multi-top final states** after LHC Run 2

EW baryogenesis in the 2HDM: a fading window?

What happens if we turn on **CP-violation**?

→ Searches for $H \to Zh$ and $A \to ZH$ probe large parts of BAU-favoured region

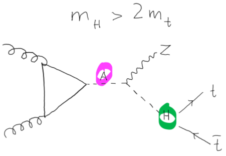

[ATLAS, 2311.04033]
[CMS, 2412.00570]

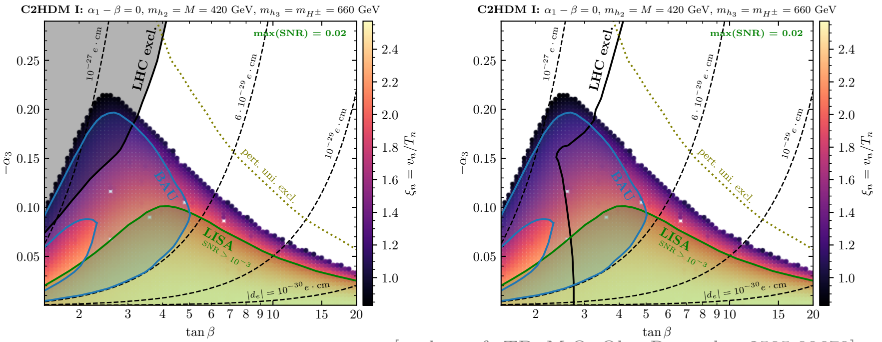

[update of: TB, M.O. Olea-Romacho, 2505.09670]

Exciting (but limited) **interplay between LHC and LISA:**

→ EW baryogenesis is possible without GW signal detectable at LISA

→ GW signal detectable at LISA does not imply discovery of new particles at LHC

Elephant in the room: BAU vs. **eEDM** constraints → tension of an order of magnitude or more

Top-quark spin correlations and angular variables

$A \to ZH \to Zt\bar{t}$:

promising probe of so far unexplored 2HDM regions compatible with EW baryogenesis

Current analyses (ATLAS/CMS): [ATLAS, 2311.04033] [CMS, 2412.00570]

cannot distinguish $A \to ZH$ vs. $H \to ZA$ and no sensitivity to **CP violation**

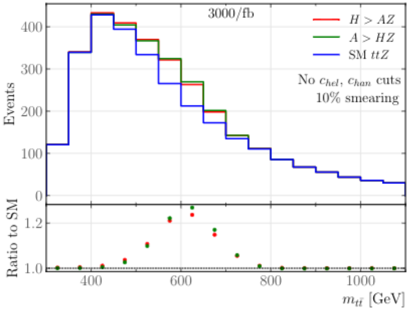

Use $t\bar{t}$ spin correlations

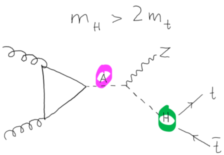

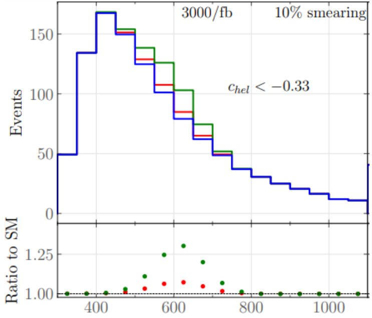

[F. Arco, TB, P. Stylianou, G. Weiglein, 2502.03443]

Top-quark spin correlations and angular variables

Lifetime of top quarks: $\tau = 0.5 \cdot 10^{-25}$ s $\to$ Decays before hadronization and spin de-correlation

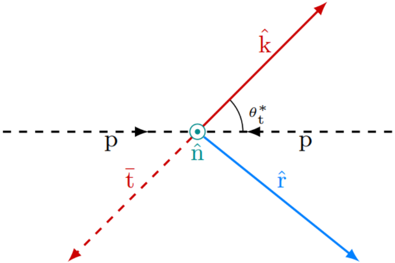

Spin density matrix of $t\bar{t}$ sub-system:

$$R \propto A\,\mathbb{1} \otimes \mathbb{1} + B_i^+ \sigma^i \otimes \mathbb{1} + B_i^- \mathbb{1} \otimes \sigma^i + C_{ij}\sigma^i \otimes \sigma^j$$

Differential cross section:

$$\frac{1}{\sigma}\frac{d\sigma}{d\cos\theta_{\hat{a}}^+ \, d\cos\theta_{\hat{b}}^+} = \frac{1}{4}(1 + B_{\hat{a}}^+ \cos\theta_{\hat{a}}^+ + B_{\hat{a}}^- \cos\theta_{\hat{a}}^- - C_{\hat{a}\hat{b}} \cos\theta_{\hat{a}}^+ \cos\theta_{\hat{b}}^-)$$

"Angles of leptons": $\cos\theta_{\hat{a}}^{\pm} = \pm \ell^{\pm} \cdot \hat{a}$

$\ell^{\pm}$ are direction of flights of leptons in their respective parent top-quark restframe, and $\hat{a} \in \{\hat{k}, \hat{r}, \hat{n}\}$

$$c_{hel} = -\cos\theta_{\hat{k}}^+ \cos\theta_{\hat{k}}^- - \cos\theta_{\hat{r}}^+ \cos\theta_{\hat{r}}^- - \cos\theta_{\hat{n}}^+ \cos\theta_{\hat{n}}^- = \hat{\ell}_t^+ \cdot \hat{\ell}_{\bar{t}}^-$$

$$c_{han} = \cos\theta_{\hat{k}}^+ \cos\theta_{\hat{k}}^- - \cos\theta_{\hat{r}}^+ \cos\theta_{\hat{r}}^- - \cos\theta_{\hat{n}}^+ \cos\theta_{\hat{n}}^-$$

c_{hel}: [Bernreuther, Heisler, Si, 1508.05271], c_{han}: [Aguilar-Saavedra, Casas, 2205.00542],

$Zt\bar{t}$ SM: [Ravina, Simpson, Howarth, 2106.09690]

A benchmark scenario at the HL-LHC

2HDM parameter points with **same total cross section**: $\mathrm{BP}_{H\to ZA}$ and $\mathrm{BP}_{A\to ZH}$

	$\mathrm{BP}_{H\to ZA}$	$\mathrm{BP}_{A\to ZH}$
$\tan\beta$	1.14	1.50
$\cos(\beta-\alpha)$	0	0
m_h/GeV	125	125
m_H/GeV	800	600
m_A/GeV	600	800
$m_{H^\pm}/\mathrm{GeV}$	800	800
M/GeV	600	600
$\mathrm{BR}(H\to t\bar t)$	71%	99%
$\mathrm{BR}(A\to t\bar t)$	99%	63%
$\mathrm{BR}(H\to ZA)$	29%	–
$\mathrm{BR}(A\to ZH)$	–	37%
Γ_H/m_H	4.3%	1.5%
Γ_A/m_A	3.5%	3.3%
$\sigma(gg\to H)/\mathrm{pb}$	0.35	0.89
$\sigma(gg\to A)/\mathrm{pb}$	2.43	0.27

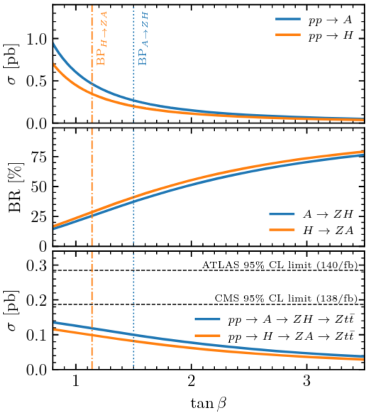

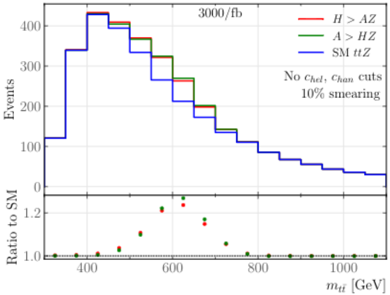

[F. Arco, TB, P. Stylianou, G. Weiglein, 2502.03443]

→ **no distinction without spin-correlation from $t\bar t$ system**

A benchmark scenario at the HL-LHC

2HDM parameter points with **same total cross section**: $\text{BP}_{H\to ZA}$ and $\text{BP}_{A\to ZH}$

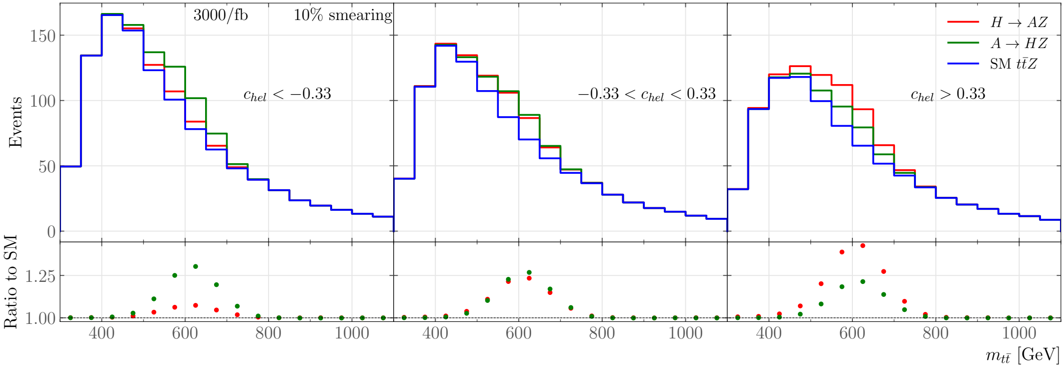

With binning in c_{hel} the two signals become distinguishable:

→ $\text{BP}_{A\to ZH}$: higher event yield for $c_{hel} < -0.33$

→ $\text{BP}_{H\to ZA}$: higher event yield for $c_{hel} > -0.33$

[F. Arco, TB, P. Stylianou, G. Weiglein, 2502.03443]

A benchmark scenario at the HL-LHC

2HDM parameter points with **same total cross section**: $\text{BP}_{H\to ZA}$ and $\text{BP}_{A\to ZH}$

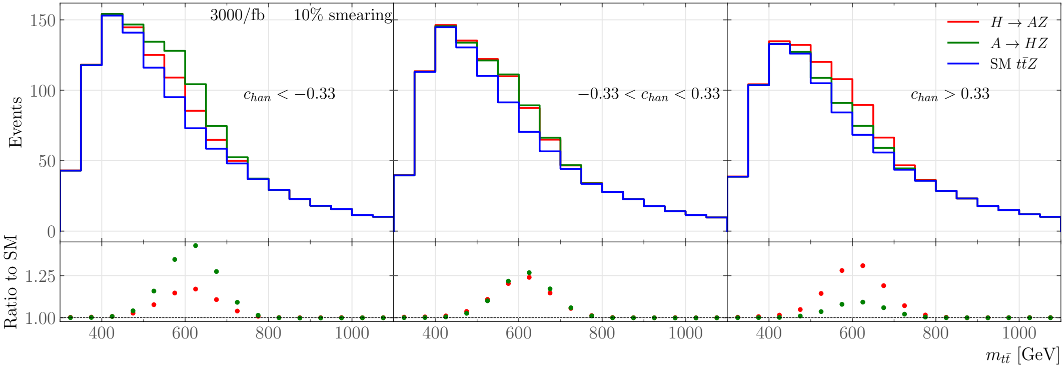

With binning in c_{han} the two signals become distinguishable:

$\to$ $\text{BP}_{A\to ZH}$: higher event yield for $c_{han} < -0.33$

$\to$ $\text{BP}_{H\to ZA}$: higher event yield for $c_{han} > -0.33$

[F. Arco, TB, P. Stylianou, G. Weiglein, 2502.03443]

Non-resonant Higgs boson pair production

A strong EWPT requires sizable modifications to the Higgs potential
$\rightarrow$ in many models correlated with **enhancements of Higgs-boson self coupling**: $\kappa_\lambda > 1$

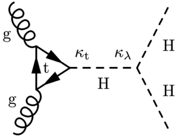

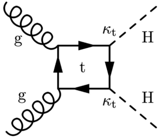

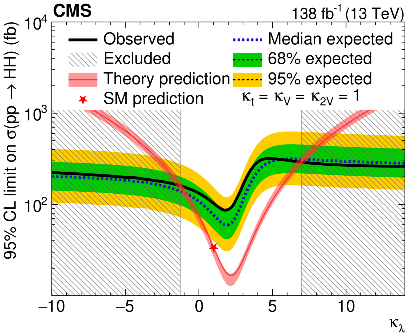

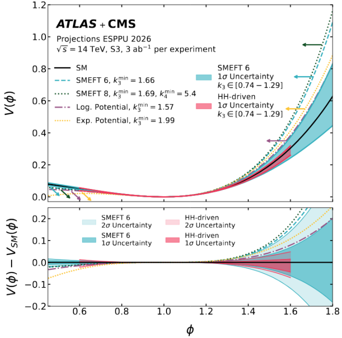

[CMS, 2510.07527] [ATLAS+CMS, 2504.00672]

Important remark: this connection holds only if the EWPT is driven by a single field direction
$\rightarrow$ counterexamples with $\kappa_\lambda \approx 1$ exist already in simplest SM extension: SM + scalar singlet

[A. Ashoorioon, T. Konstandin, 0904.0353], [D. Curtin, P. Meade, C.T. Yu, 1409.0005]

Non-resonant Higgs boson pair production

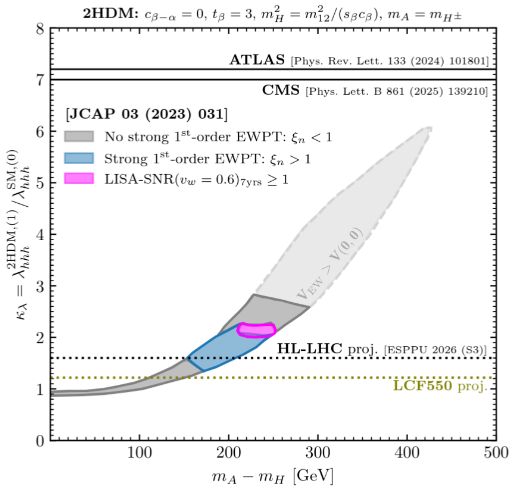

based on [TB, Heinemeyer, No, Olea-Romacho, Weiglein, 2208.14466], prepared for [LC vision collab., 2503.19983]

Representative benchmark scenario in the alignment limit of the 2HDM

→ Crucial to place LISA expectations in the context of HL-LHC prospects

→ Future e^+e^- collider could probe the entire region predicting a strong EWPT

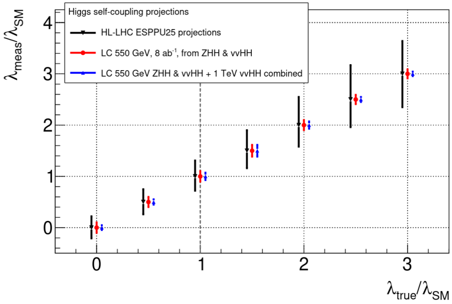

[LC vision collab., 2503.19983]

A (collider) nightmare scenario

Add a gauge-singlet scalar with "dark" $\mathbb{Z}_2$: $V = V_{\mathrm{SM}} + \frac{1}{2}\mu_s^2|S|^2 + \frac{1}{4}\lambda_s|S|^4 + \frac{1}{2}\lambda_{hs}|S|^2 H^\dagger H$

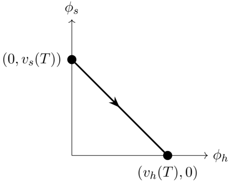

For $\mu_s^2 < 0$: strong EWPT with $T = 0$ Higgs potential SM-like

$\rightarrow$ $\delta\kappa_\lambda$ can remain well below 10%

$\rightarrow$ rel. corrections to $\sigma(e^+e^- \rightarrow Zh)$ at permille level

[D. Curtin, P. Meade, C.T. Yu, 1409.0005]

LISA possibly the only way to test this scenario in the foreseeable future

But: **Theoretical uncertainties** of GW predictions have to be reduced

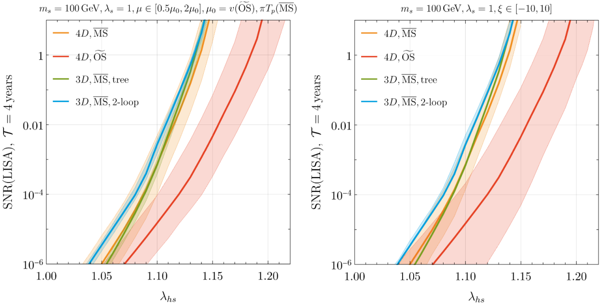

[TB, A. Dashko, M. Löschner, G. Weiglein, 2511.14831]

From BSM theory to GW signal

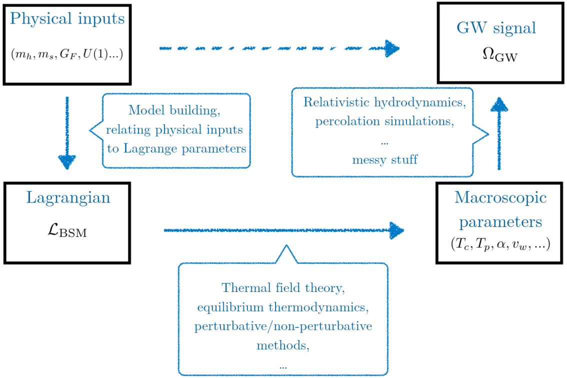

High-temperature EFT:

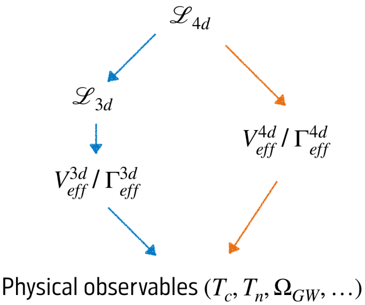

[Andrii Dashko, PASCOS '25]

There are sizable theoretical uncertainties in all of the above steps

Rapidly evolving field: *"gold rush"* for theorists

Perturbative methods and renormalization schemes

"4D approach": Working in full 4D UV theory

$$V_{\rm eff}(\Phi, T, \mu, \xi) = V_{\rm tree}(\Phi) + V_{\rm CW}^{(1)}(\Phi, \mu, \xi) + V_T^{(1)}(\Phi, T, \xi) + V_{\rm AE}(\phi, T, \xi)$$

- Thermal corrections via explicit T-dependence in $V_{\rm eff}$
- $\overline{\rm MS}$-scheme: one-loop corrected parameter relations, e.g. $\mu_h^2(\mu) = -[m_h^2 + \Sigma_h(p^2 = m_h^2, \mu)]/2$
- OS-like scheme $\widetilde{\rm OS}$: add counterterm potential $V_{\rm CT}(\mu, \xi)$ satisfying $\partial_{\phi_i} V_{\rm CW} = -\partial_{\phi_i} V_{\rm CT}$, $\partial_{\phi_i}\partial_{\phi_j} V_{\rm CW} = -\partial_{\phi_i}\partial_{\phi_j} V_{\rm CT}$
- Ad-hoc resummation of large IR divergent corrections via $V_{\rm AE}$

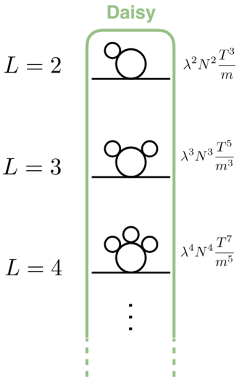

[Curtin, Meade, Ramani, 1612.00466]

"3D approach": integrating out non-zero Matsubara modes

$$V_{\rm eff}^{3D}(\Phi, \mu, \mu_{3D}, \xi) = V_0^{3D}(\Phi) + V_1^{3D}(\Phi, \xi) + V_2^{3D}(\Phi, \mu_{3D}, \xi)$$

- Resulting EFT lives in 3 spatial dimensions ($T \sim \tau = it$ integrated out)
- Only bosonic zero modes are dynamical fields
- Thermal corrections via implicit T-dependence in matching relations, e.g. LO matching: $\mu_{h,3D}^2 = \mu_h^2 + T^2(3g_1^2 + 9g_2^2 + 12y_t^2 + 2\lambda_{hs} + 24\lambda_s)/48$

[TB, A. Dashko, M. Löschner, G. Weiglein, 2511.14831]

EWPT in the cxSM: scale dependence

4D approach: Explicit renormalization scale dependence

3D approach: Implicit (hard) matching scale dependence from truncation of matching

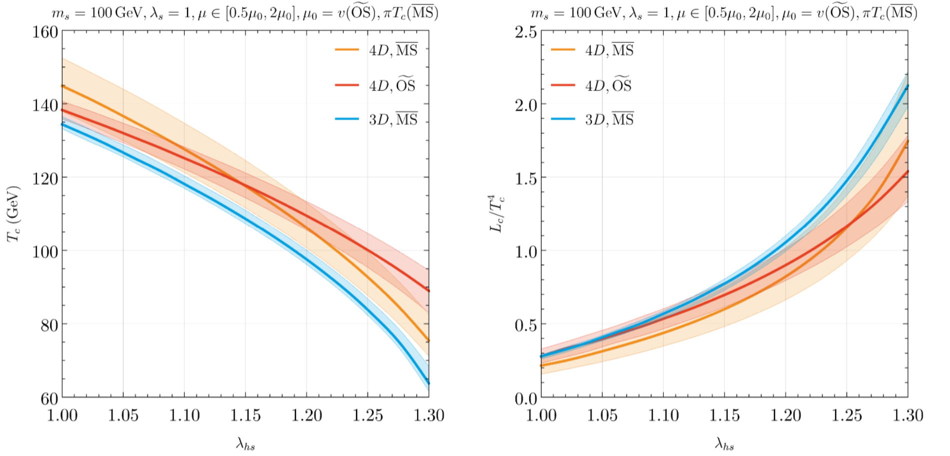

[TB, A. Dashko, M. Löschner, G. Weiglein, 2511.14831]

EWPT in the cxSM: gauge dependence

Gauge dependence governed by Nielson Identity: $\xi \frac{\partial}{\partial \xi} V(\Phi, \xi) = C(\Phi, \xi) \frac{\partial}{\partial \Phi} V(\Phi, \xi)$

Gauge-independent results with "$\hbar$-expansion" [Fukuda, Kugo (1976), Patel, Ramsey-Musolf, 1101.4665]

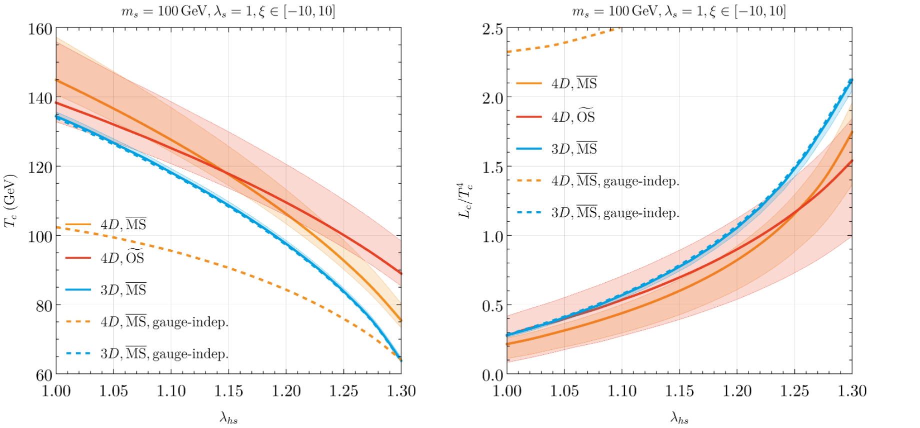

Results using "background R_ξ-gauge" [TB, A. Dashko, M. Löschner, G. Weiglein, 2511.14831]

GW in the cxSM: Theory uncertainties

Scale and gauge dependence give rise to **order-of-magnitude** uncertainties in the LISA SNR
Significantly reduced theory uncertainties in the 3D approach

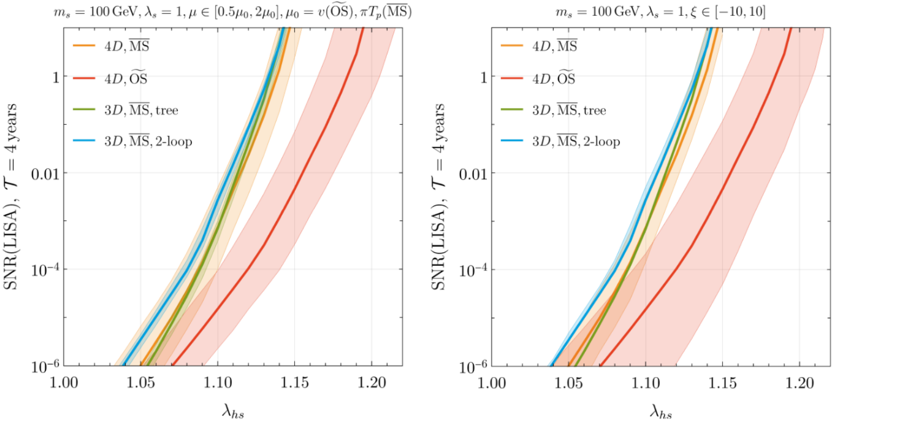

[TB, A. Dashko, M. Löschner, G. Weiglein, 2511.14831]

Echoes of an EWPT at LISA

Model parameters (masses, couplings) $\leftrightarrow$ $V_{\rm eff}(\phi_i)$ $\leftrightarrow$ PT characteristics $\leftrightarrow$ GW signal $h^2\Omega$

[LISA-COSWG-24-01], [TB, 2507.06082], [TB, A. Dashko, K. Radchenko, WIP]

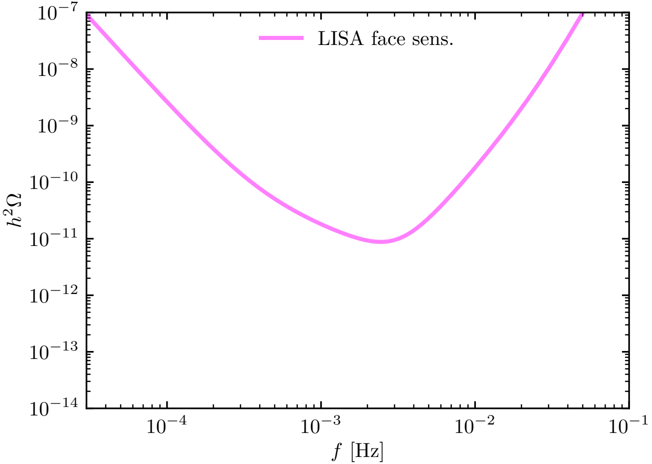

LISA senitivity curve

Echoes of an EWPT at LISA

Model parameters (masses, couplings) $\leftrightarrow V_{\rm eff}(\phi_i) \leftrightarrow$ PT characteristics $\leftrightarrow$ GW signal $h^2\Omega$

[LISA-COSWG-24-01], [TB, 2507.06082], [TB, A. Dashko, K. Radchenko, WIP]

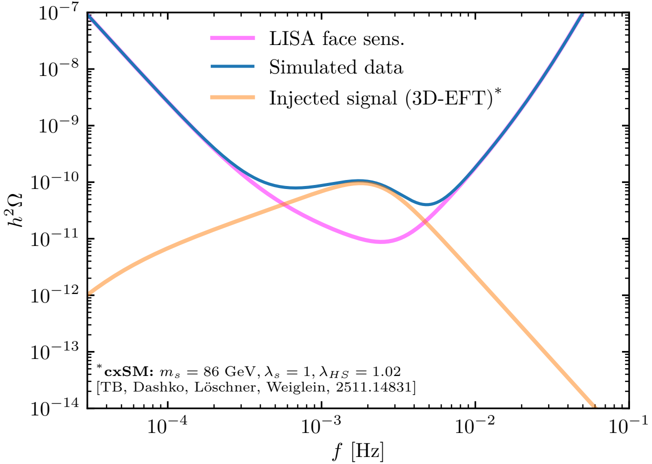

GW signal from an EWPT in an ideal world

Echoes of an EWPT at LISA

Model parameters (masses, couplings) $\leftrightarrow V_{\text{eff}}(\phi_i) \leftrightarrow$ PT characteristics $\leftrightarrow$ GW signal $h^2\Omega$

[LISA-COSWG-24-01], [TB, 2507.06082], [TB, A. Dashko, K. Radchenko, WIP]

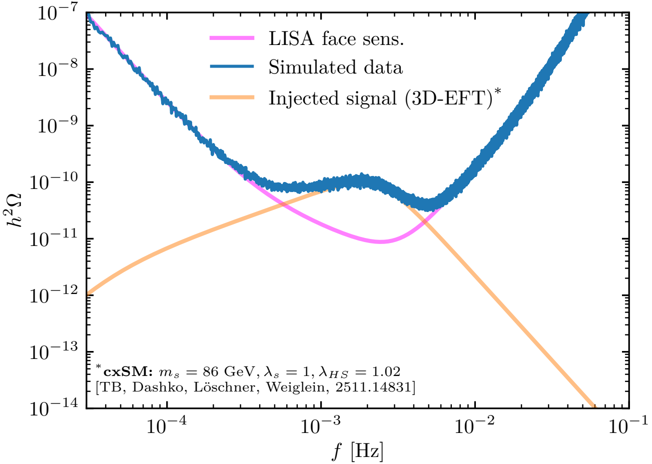

GW signal from an EWPT in the real world: instrumental noise

Echoes of an EWPT at LISA

Model parameters (masses, couplings) $\leftrightarrow V_{\text{eff}}(\phi_i) \leftrightarrow$ PT characteristics $\leftrightarrow$ GW signal $h^2\Omega$

[LISA-COSWG-24-01], [TB, 2507.06082], [TB, A. Dashko, K. Radchenko, WIP]

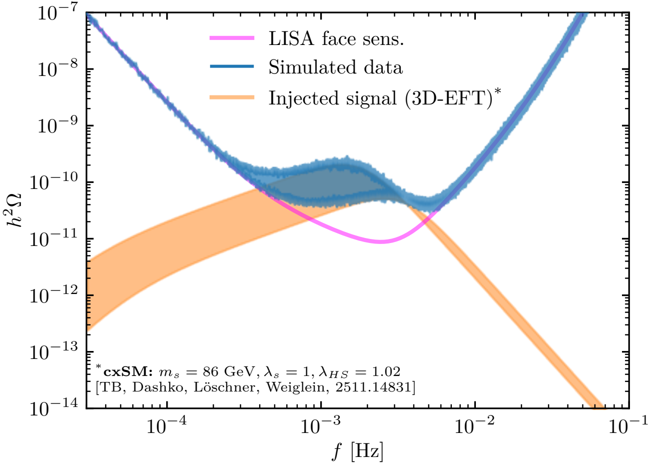

Theoretical uncertainties in $V_{\text{eff}}(\phi_i)$: scale dependence

Echoes of an EWPT at LISA

Model parameters (masses, couplings) $\leftrightarrow$ $V_{\text{eff}}(\phi_i)$ $\leftrightarrow$ PT characteristics $\leftrightarrow$ GW signal $h^2\Omega$

[LISA-COSWG-24-01], [TB, 2507.06082], [TB, A. Dashko, K. Radchenko, WIP]

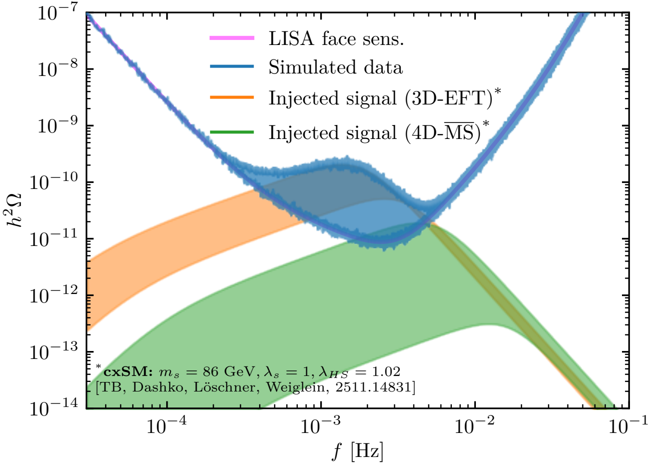

Ambiguities: high-T 3D-EFT (two-loop matching) vs. full model 4D-$\overline{\text{MS}}$ (one-loop)

Echoes of an EWPT at LISA

Model parameters (masses, couplings) $\leftrightarrow V_{\text{eff}}(\phi_i) \leftrightarrow$ PT characteristics $\leftrightarrow$ GW signal $h^2\Omega$

[LISA-COSWG-24-01], [TB, 2507.06082], [TB, A. Dashko, K. Radchenko, WIP]

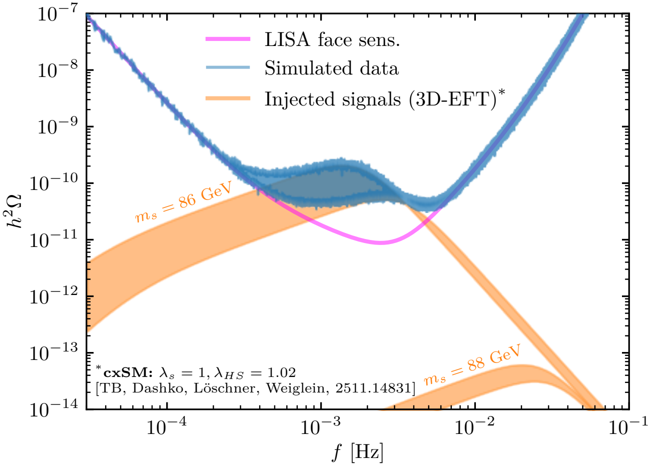

Parametric uncertainties: strong sensitivity on underlying model parameters

Echoes of an EWPT at LISA

Model parameters (masses, couplings) $\leftrightarrow V_{\text{eff}}(\phi_i) \leftrightarrow$ PT characteristics $\leftrightarrow$ GW signal $h^2\Omega$

[LISA-COSWG-24-01], [TB, 2507.06082], [TB, A. Dashko, K. Radchenko, WIP]

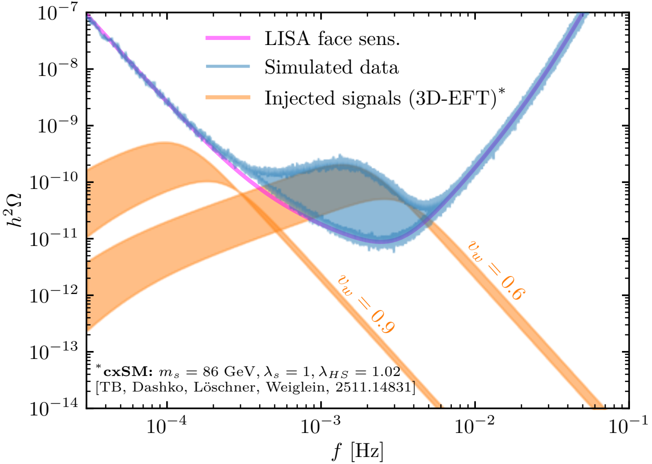

Parametric uncertainties: no precise prediction for the bubble wall velociy v_w

EW baryogenesis without tension with eEDM limits

Sizable CP-violation (CPV) for EW baryogenesis while **evading the constraints from EDMs**:

1. Parameter tuning
→ accidental cancellation in eEDM

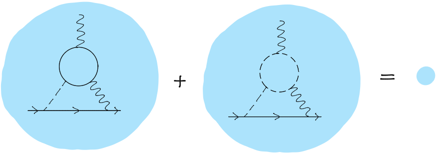

2. Suppression of electron Yukawa
→ CPV decoupled from eEDM

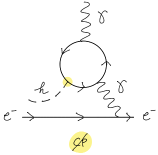

3. Secluded CPV
→ CPV interactions with “dark sector”

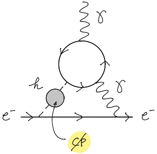

4. Transient CPV
→ Primordial CPV enhanced at $T > 0$

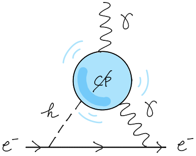

[Drawings by Kateryna Radchenko]

Realization of secluded + transient CP-violation

2HDM+S2: 2HDM + real scalar singlet with “dark” $\mathbb{Z}_2$ symmetry

Thermal history: $T \sim 100$ GeV $\rightarrow$ **transient** enhancement of CP-violation during EWPT
$T = 0$ GeV $\rightarrow$ “dark” $\mathbb{Z}_2$ restored and CP-violation is **secluded**

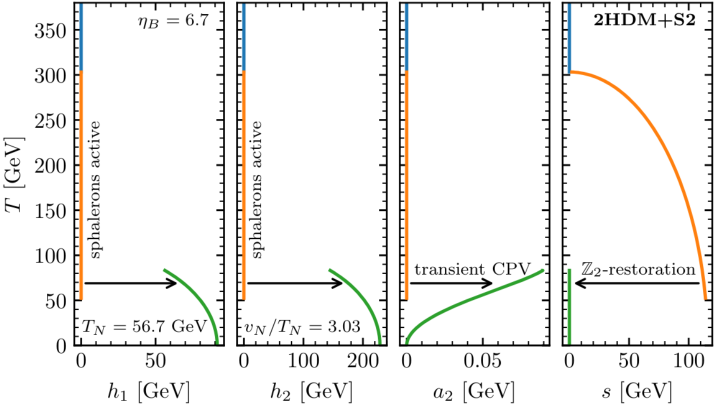

h_1: CP-even Higgs vev
h_2: CP-even Higgs vev
a_2: CP-odd Higgs vev
s: singlet vev

eEDM at 3-loop level:

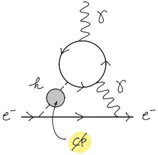

[TB, J. Cano, S. Gori, K. Mimasu, J.M. No, to be published]

2HDM+S2: LHC signatures

Transient CP-violation favours a rather **light singlet scalar**: $m_{A_0}, m_{H_0} \gtrsim 2m_S$

→ **LHC phenomonology:** 2HDM with extra invisible decays of BSM neutral scalars

Magenta: BAU-favoured region

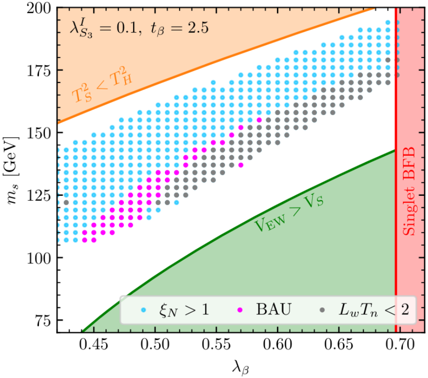

Exclusions from CM mono-jet search:

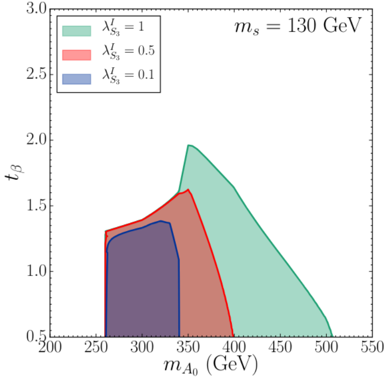

[TB, J. Cano, S. Gori, K. Mimasu, J.M. No, to be published]

Recasting of [CMS, 2107.130221]

Complementary limits from **mono-jet/Z/H searches** vs. searches without missing E_T

The road ahead

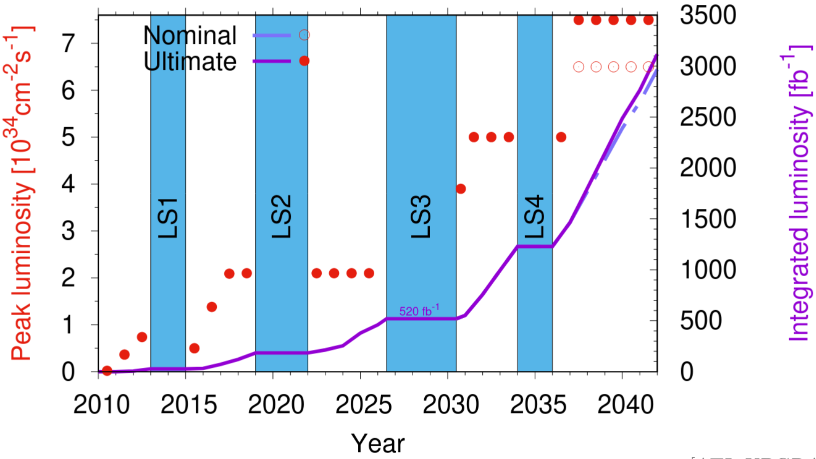

[ATL-UPGRADE-PUB-2025]

The road ahead

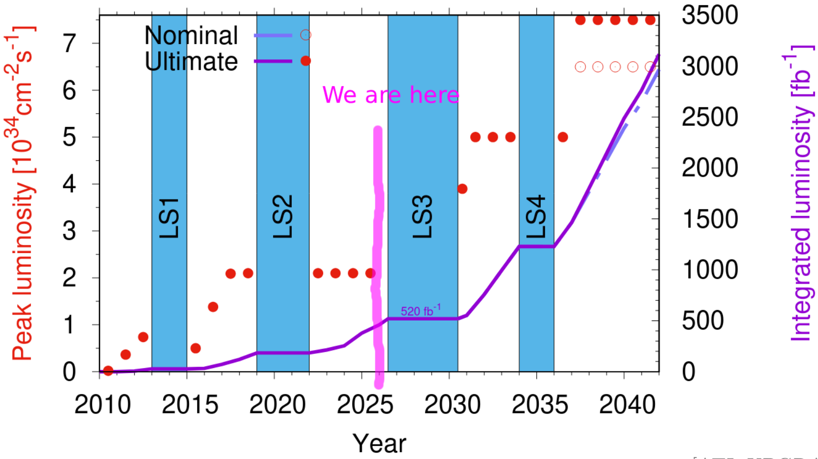

[ATL-UPGRADE-PUB-2025]

The road ahead

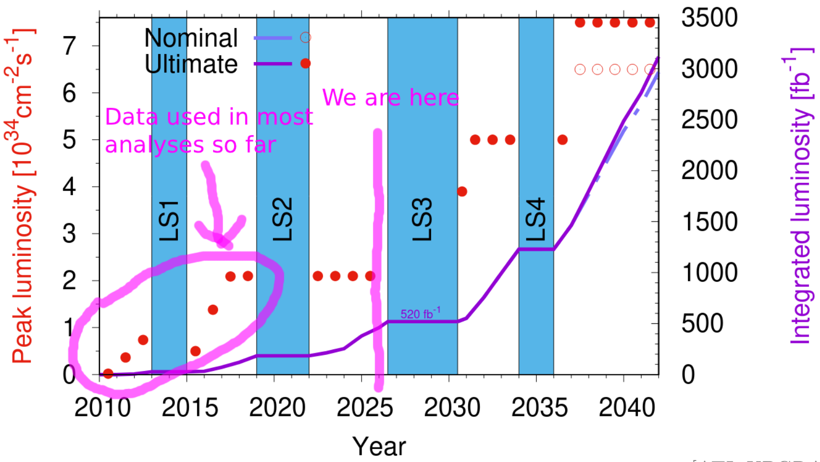

[ATL-UPGRADE-PUB-2025]

The road ahead

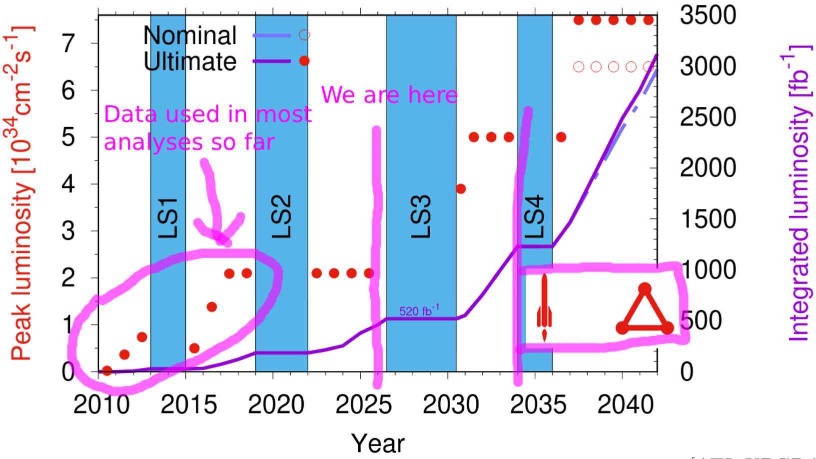

[ATL-UPGRADE-PUB-2025]

Thanks!

EW baryogenesis in the C2HDM

Minimal scenario for EW baryogenesis: Complex 2HDM (C2HDM), softly broken $\mathbb{Z}_2$

Benchmark planes for LHC searches:

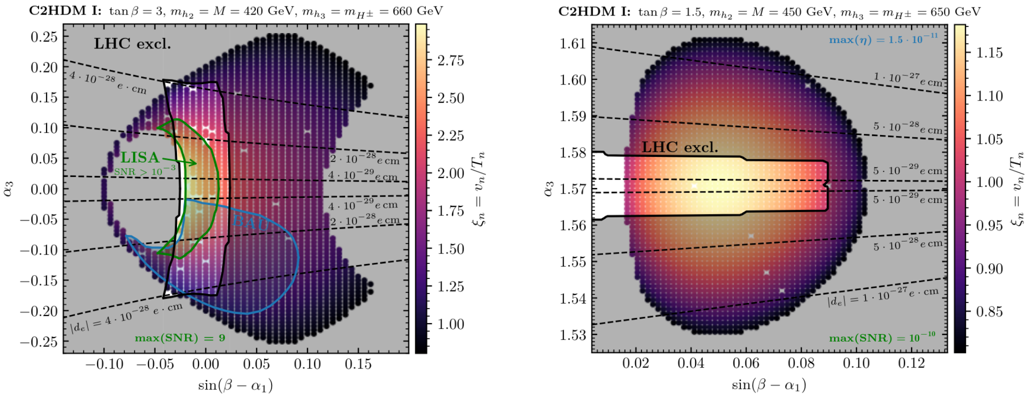

[TB, M.O. Olea-Romacho, 2505.09670]

Exclusion regions from smoking gun: Type I/II

Impact of searches for $pp \to A \to ZH \to Zt\bar{t}$ [ATLAS, 2311.04033]

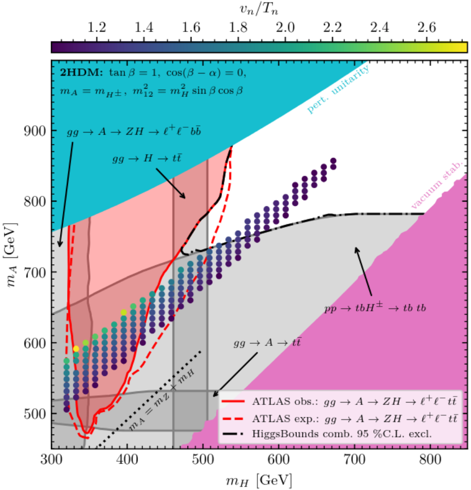

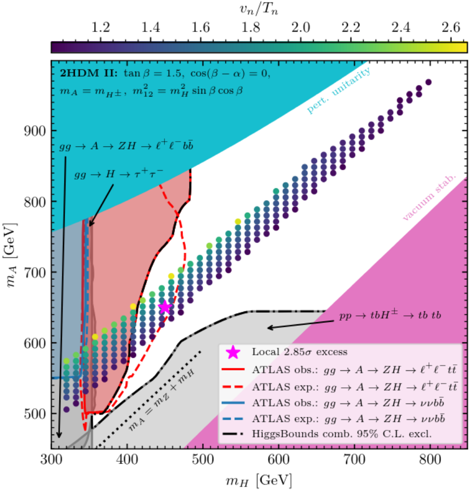

[TB, Heinemeyer, Olea-Romacho, No, Radchenko, Weiglein, 2309.17431]

Exclusion regions from smoking gun: Type IV

Impact of searches for $pp \to A \to ZH \to Zt\bar{t}$ [ATLAS, 2311.04033]

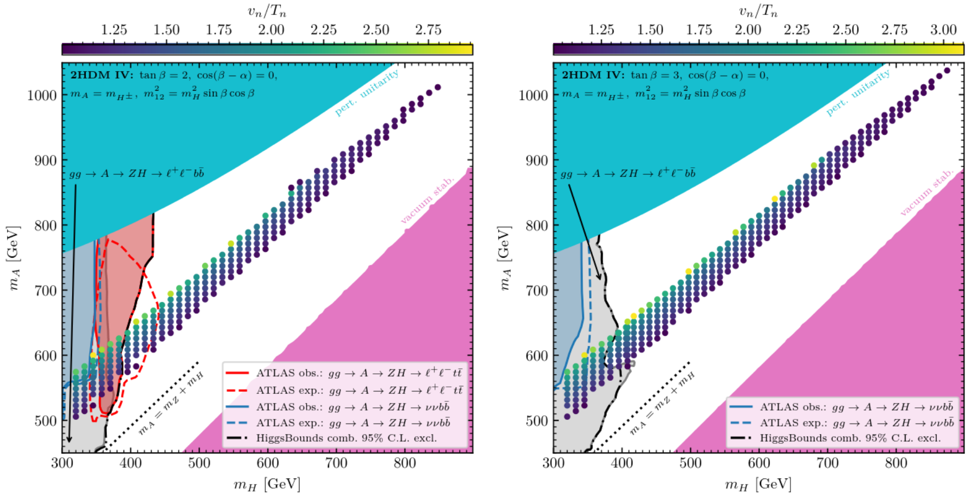

[TB, Heinemeyer, Olea-Romacho, No, Radchenko, Weiglein, 2309.17431]

Monte Carlo simulation: Signal

$$gg \to \begin{pmatrix} A \\ H \end{pmatrix} \to \begin{pmatrix} ZH \\ ZA \end{pmatrix} \to Z\,t\bar{t} \to \ell^+\ell^-\, b\bar{b}\ell^+\ell^-\nu_\ell\bar{\nu}_\ell$$

- $gg \to A/H$ cross sections simulated at LO with MadGraph5_aMC@NLO
- LO Agg/Hgg vertices implemented in UFO with FeynRules including p^2-dependence:

$$\mathcal{L} \supset \frac{\alpha_S}{8\pi v}\left[\mathcal{F}_H(\tau) H G^a_{\mu\nu} G^{a\mu\nu} + i\mathcal{F}_A(\tau) A G^a_{\mu\nu} \widetilde{G}^{a\mu\nu}\right], \quad \tau = \frac{\hat{s}}{4m_t^2}$$

- NNLO QCD K-factor from HiggsTools/SusHi
- Decays $A/H \to t\bar{t}$ and $A \to ZH/H \to ZA$ from:

$$\mathcal{L} \supset -\frac{m_t}{v t_\beta}\bar{t}(H + iA\gamma_5)t - \frac{e}{2 s_W c_W}(H\partial_\mu A - A\partial_\mu H)Z^\mu$$

- HDECAY for total width of heavier resonance includes NLO QCD and off-shell corrections

[F. Arco, TB, P. Stylianou, G. Weiglein, 2502.03443]

Background, cuts and efficiency factors

The main **background** in the fully leptonic channel is $pp \to Zt\bar{t}$ production:

- Simulated at LO with MadGraph5_aMC@NLO (leptonic decays: $t \to b\ell\nu_\ell$ and $Z \to \ell^+\ell^-$)
- Background normalization factor to obtain the same number of total background events as ATLAS in their measurement of SM $Zt\bar{t}$ production [2312.04450] (which includes additional minor backgrounds)

Cuts following ATLAS measurement of SM $Zt\bar{t}$ production [2312.04450]:

- Selected leptons are required to have $p_T(\ell) > 10$ GeV, $|\eta(\ell)| < 2.5$
- We require two pairs of OSSF leptons, with the leading lepton having $p_T(\ell) > 27$ GeV
- One lepton pair with invariant mass $m_{\ell\ell}$ close to m_Z: $|m_Z - m_{\ell\ell}| < 20$ GeV
- We require at least two b-jets with $p_T(j) > 25$ GeV and $|\eta(j)| < 2.5$

Efficiency factors to better simulate real experimental analysis:

- 10% gaussian smearing (for HL-LHC) to simulate detector response
- Efficiency factor of $(0.7)^2$ for b-tagging of jets
- Efficiency factor of 0.9 to account for reconstruction of top quarks

[F. Arco, TB, P. Stylianou, G. Weiglein, 2502.03443]

Top-quark spin correlations and angular variables

$$c_{hel} = -\cos\theta^+_{\hat{k}}\cos\theta^-_{\hat{k}} - \cos\theta^+_{\hat{r}}\cos\theta^-_{\hat{r}} - \cos\theta^+_{\hat{n}}\cos\theta^-_{\hat{n}} = \hat{\ell}^+_t \cdot \hat{\ell}^-_{\bar{t}}$$

$$c_{han} = \cos\theta^+_{\hat{k}}\cos\theta^-_{\hat{k}} - \cos\theta^+_{\hat{r}}\cos\theta^-_{\hat{r}} - \cos\theta^+_{\hat{n}}\cos\theta^-_{\hat{n}}$$

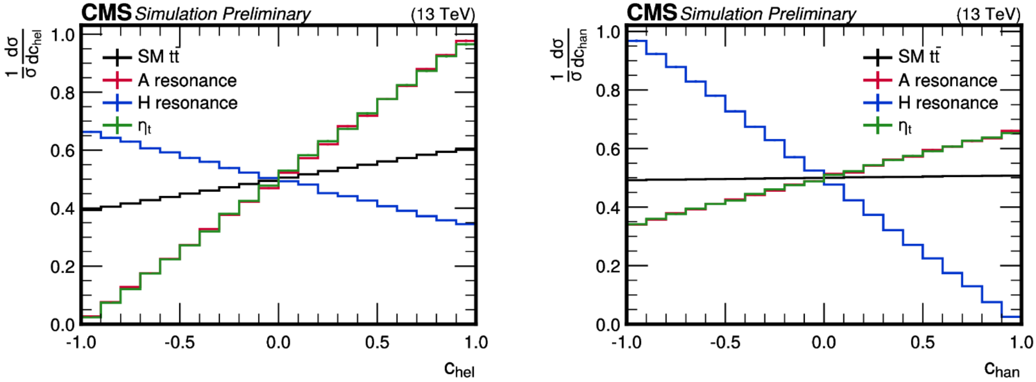

[CMS-PAS-HIG-22-013]

Results: Angular distributions

Binning events in c_{hel} and c_{han}: (a.u.: arbitrary units)

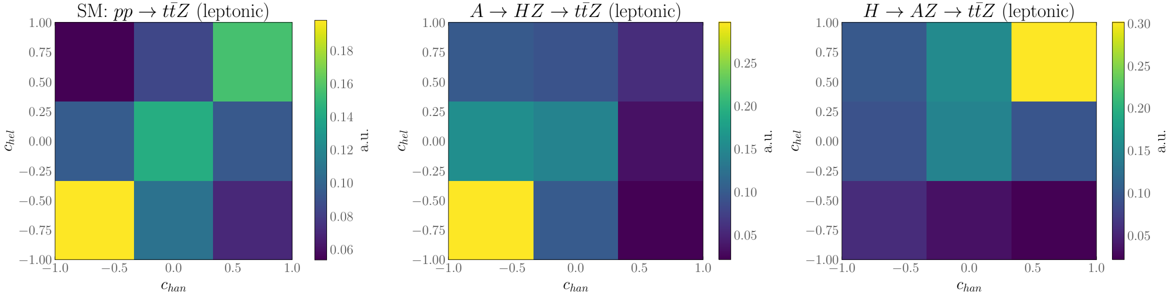

The two signals are potentially distinguishable:

$\Rightarrow$ $A \to ZH$ peaks in negative c_{hel} and c_{han} bin

$\Rightarrow$ $H \to ZA$ peaks in positive c_{hel} and c_{han} bin

[F. Arco, TB, P. Stylianou, G. Weiglein, 2502.03443]

Results: benchmark scenario at the HL-LHC

$m_{t\bar{t}}$ distribution in different c_{hel} bins:

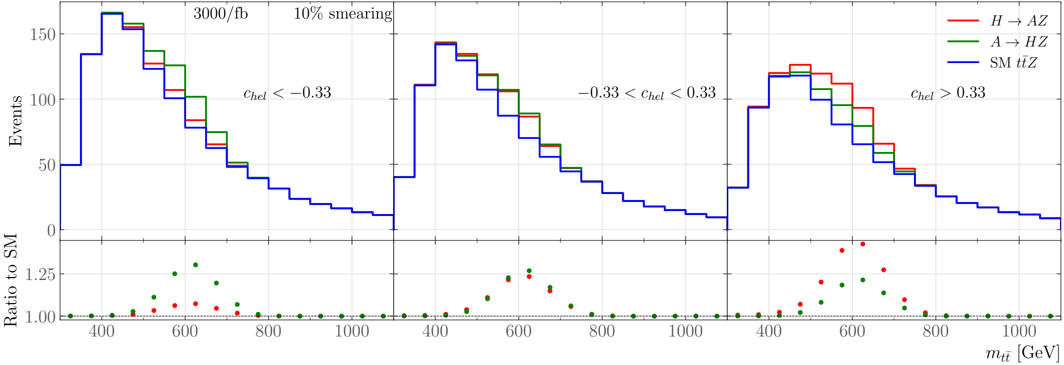

[F. Arco, TB, P. Stylianou, G. Weiglein, 2502.03443]

Results: benchmark scenario at the HL-LHC

$m_{t\bar{t}}$ distribution in different c_{han} bins:

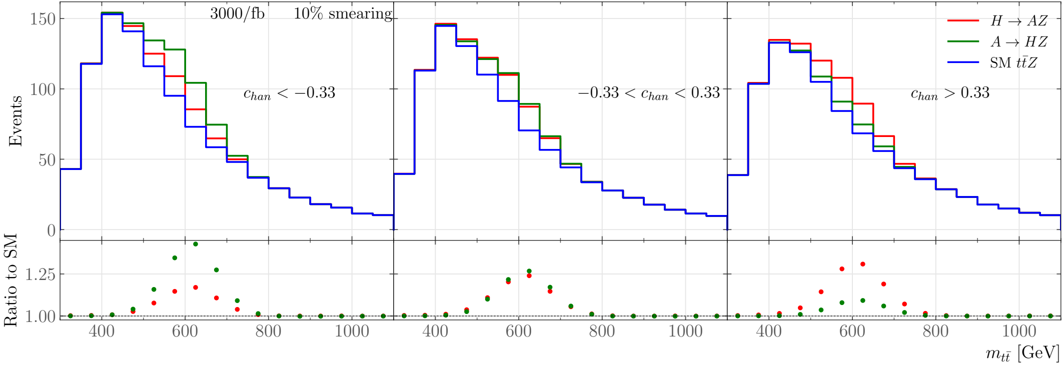

[F. Arco, TB, P. Stylianou, G. Weiglein, 2502.03443]

Dimensional reduction

We used `DRalgo` to carry out dimensional reduction at two-loop level

[Ekstedt, Schicho, Tenkanen, 2205.08815]

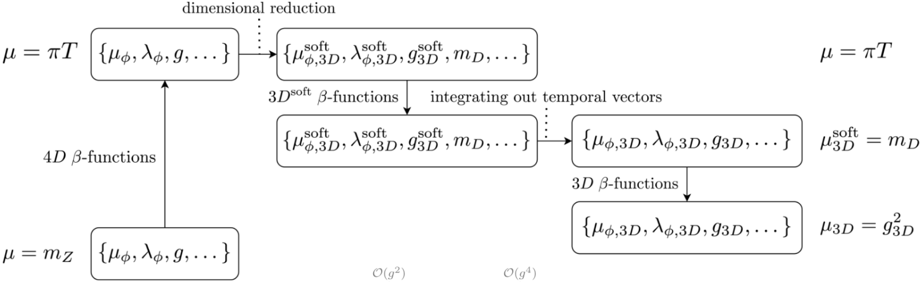

$$\mu^2_{\phi,3D} = \overbrace{\underbrace{\mu_\phi^2}_{\text{tree}} + \#g^2T^2}^{\mathcal{O}(g^2)} + \overbrace{\#g^2\mu_\phi^2 + \underbrace{\#g^4T^2}_{\text{2-loop}}}^{\mathcal{O}(g^4)} + \mathcal{O}(g^6)\,, \qquad \underbrace{\#g^2T^2 + \#g^2\mu_\phi^2}_{\text{1-loop}}$$

$$\lambda_{\phi,3D} = \overbrace{\underbrace{\lambda_\phi T}_{\text{tree}}}^{\mathcal{O}(g^2)} + \overbrace{\underbrace{\#g^4T}_{\text{1-loop}}}^{\mathcal{O}(g^4)} + \mathcal{O}(g^6)\,,$$

[TB, Dashko, Löschner, Weiglein, 2511.14831]

$$g^2_{3D} = \overbrace{\underbrace{g^2T}_{\text{tree}}}^{\mathcal{O}(g^2)} + \overbrace{\underbrace{\#g^4T}_{\text{1-loop}}}^{\mathcal{O}(g^4)} + \mathcal{O}(g^6)\,,$$

hbar-expansion

Instead of numerical minimzation of potential: [Fukuda, Kugo (1976), Patel, Ramsey-Musolf, 1101.4665]

$$V(\phi) = V_0(\phi) + \hbar V_1(\phi) + \hbar^2 V_2(\phi) + \mathcal{O}(\hbar^3)\,, \tag{3.13}$$

$$v = v_0 + \hbar v_1 + \hbar^2 v_2 + \mathcal{O}(\hbar^3)\,. \tag{3.14}$$

Extremizing the potential and collecting contributions in terms of powers of $\hbar$ result in

$$\begin{aligned} 0 = \partial_\phi V_0\big|_{v_0} + \hbar\left[\partial_\phi V_1 + v_1 \partial_\phi^2 V_0\right]\Big|_{v_0} \\ + \hbar^2\left[\partial_\phi V_2 + v_2 \partial_\phi^2 V_0 + v_1 \partial_\phi^2 V_1 + \frac{1}{2} v_1^2 \partial_\phi^3 V_0\right]\Bigg|_{v_0} + \mathcal{O}(\hbar^3). \end{aligned} \tag{3.15}$$

This defines the tree-level extremum

$$\partial_\phi V_0\big|_{v_0} = 0\,, \tag{3.16}$$

the one-loop extremum

$$v_1 = -\frac{\partial_\phi V_1}{\partial_\phi^2 V_0}\Bigg|_{v_0}\,, \tag{3.17}$$

and the two-loop extremum

$$v_2 = \frac{-2\partial_\phi V_2 (\partial_\phi^2 V_0)^2 + 2\partial_\phi V_1 \partial_\phi^2 V_0 \partial_\phi^2 V_1 - (\partial_\phi V_1)^2 \partial_\phi^3 V_0}{2(\partial_\phi^2 V_0)^3}\Bigg|_{v_0}\,. \tag{3.18}$$

[TB, Dashko, Löschner, Weiglein, 2511.14831]

$$\mathcal{L}_{GF} = -\frac{1}{2}\left(F_\gamma^2 + F_Z^2 + 2F_W^+ F_W^-\right), \tag{4.5}$$

with

$$F_\gamma = -\frac{1}{(\xi_1^\gamma)^{1/2}}\partial^\mu A_\mu, \tag{4.6}$$

$$F_Z = -\frac{1}{(\xi_1^Z)^{1/2}}\left(\partial^\mu Z_\mu + i\xi_2^Z \frac{\sqrt{g^2+g'^2}\phi^{GF}}{2} G_0\right), \tag{4.7}$$

$$F_W^\pm = -\frac{1}{(\xi_1^W)^{1/2}}\left(\partial^\mu W_\mu^\pm \mp i\xi_2^W \frac{g\phi^{GF}}{2} G_\pm\right), \tag{4.8}$$

where $\xi_1^{Z,W,\gamma}$, $\xi_2^{Z,W}$ and ϕ_i^{GF} are the gauge-fixing parameters. We suppress the superscripts (Z, W, γ) in the following for better readability. Some commonly used choices for the gauge-fixing parameters, which we study in the presented work, are

1. **Fermi gauge**: $\xi_1 = \xi$, $\xi_2 = 0$. In this case, ghosts become massless, but calculations are complicated by the presence of mixing propagators between vector bosons and the corresponding Goldstone bosons. Moreover, infrared (IR) divergences arise, necessitating additional resummation procedures [119].

2. R_ξ**-gauges**: $\xi_1 = \xi_2 = \xi$.[17] These are usually introduced to cancel the aforementioned mixing propagators. Two subclasses can be defined here:

   (a) In the so-called *background* R_ξ-gauge, one uses $\phi^{GF} = \phi_h$. Thence, the vector-Goldstone mixing is canceled for all values of the background field ϕ_h, and ghosts become massive.

   (b) In the *standard* R_ξ-gauge, one uses $\phi^{GF} = v_h$. Here, the vector-Goldstone mixing is canceled only at the minimum field configuration $\phi_{h,\mathrm{min}} = v_h$, and the ghosts are massive. Note that in this gauge, the effective potential is not symmetric under $\phi_h \to -\phi_h$.

3. **Landau gauge** is a limit of both Fermi and R_ξ-gauges with $\xi \to 0$.[18] Ghosts are massless and mixing propagators are absent.

[TB, Dashko, Löschner, Weiglein, 2511.14831]

GWs in the cxSM: theory uncertainties

Numerical uncertainties from residual gauge dependence can be of the same size or even larger ($4D$-$\widetilde{\mathrm{OS}}$ scheme) than the ones from scale dependence:

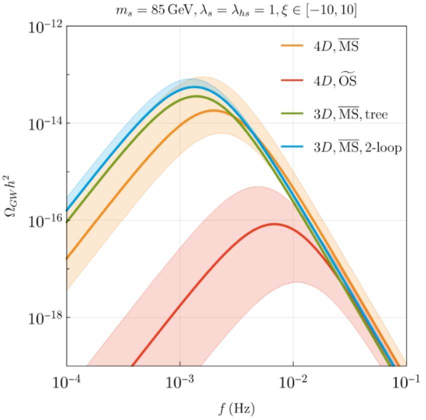

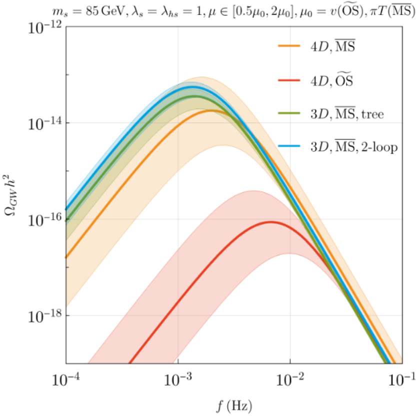

[TB, Dashko, Löschner, Weiglein, 2511.14831]

GWs in the cxSM: theory uncertainties

Application of $\hbar$-expansion gives gauge-independent predicions and is straight-forward in $3D$-EFT, but in $4D$ the $\hbar$-expansion gives rise too large discrepancies:

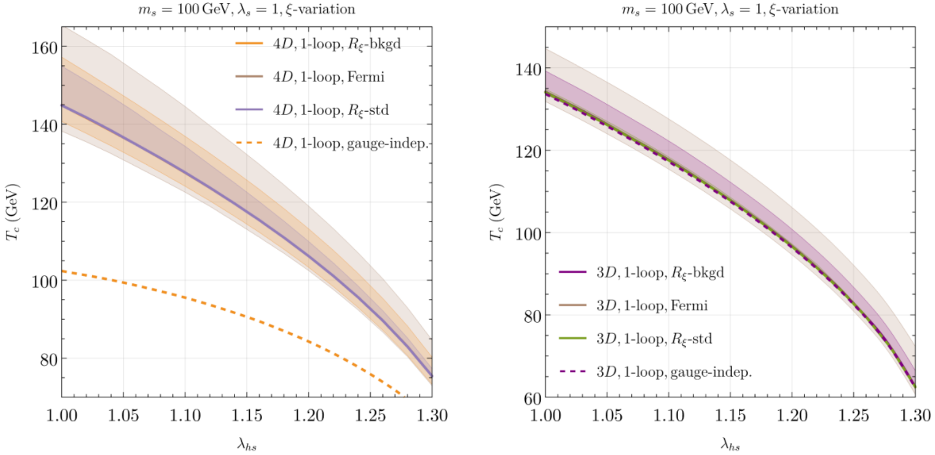

[TB, Dashko, Löschner, Weiglein, 2511.14831]

GWs in the cxSM: theory uncertainties

Parameter space regions with strongest GW signals the high-temperature expansion starts to break down. Impact of higher-dimensional operatores in 3D-EFT becomes relevant:

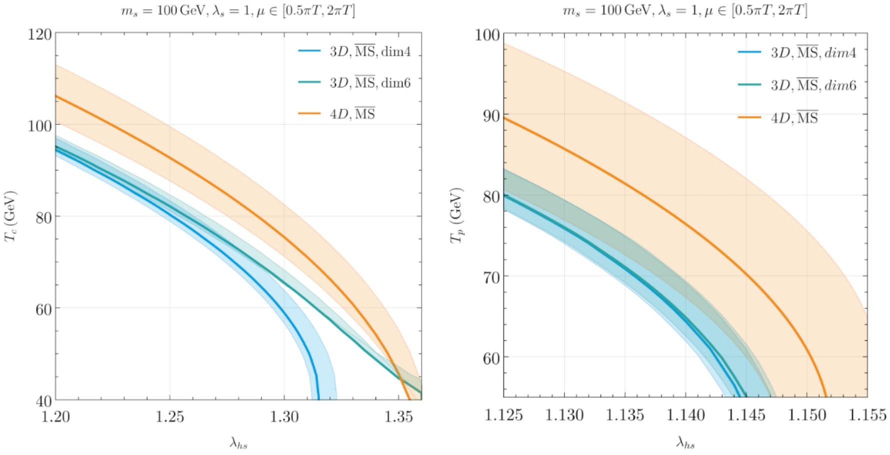

[TB, Dashko, Löschner, Weiglein, 2511.14831]

cS2HDM: Electron EDM

$$|d_e| \sim \frac{m_e}{1 \text{ MeV}} \left(\frac{1 \text{ TeV}}{M} \right)^2 \cdot 10^{-26} \ e \text{ cm}$$

eEDM can be suppressed via **cancellations**, e.g. via flavour alignment

CP-mixed state H_1 | CP-even state H_1

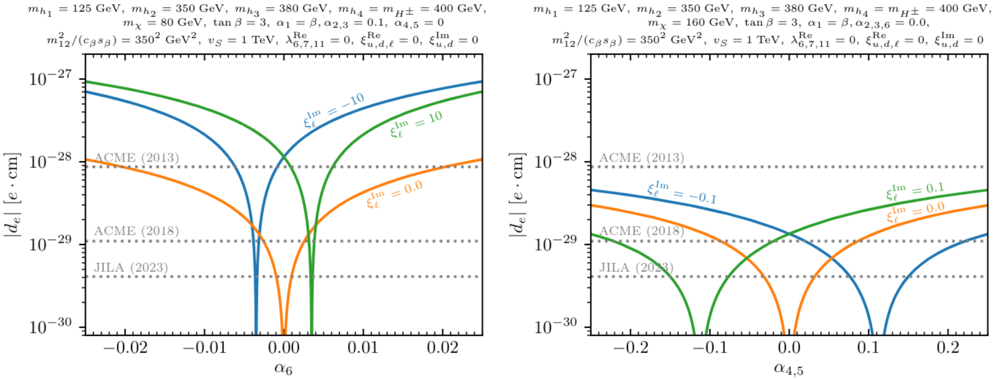

[TB, P. Gabriel, M.M. Mühlleitner, R. Santos, 2509.01682]